

Time-resolved spectroscopy of biexciton luminescence in $Zn_xCd_{1-x}Se-Zn_{1-y}SySe_y$ multiple quantum wells

著者	Yamada Yoichi, Mishina Tomobumi, Masumoto Yasuaki, Kawakami Yoichi, Yamaguchi Shigeo, Ichino Kunio, Fujita Shizuo, Fujita Shigeo, Taguchi Tsunemasa
journal or publication title	Physical review B
volume	51
number	4
page range	2596-2599
year	1995-01
権利	(C)1995 The American Physical Society
URL	http://hdl.handle.net/2241/98244

doi: 10.1103/PhysRevB.51.2596

Time-resolved spectroscopy of biexciton luminescence in $\text{Zn}_x\text{Cd}_{1-x}\text{Se-ZnS}_y\text{Se}_{1-y}$ multiple quantum wells

Yoichi Yamada, Tomobumi Mishina, and Yasuaki Masumoto
Institute of Physics, University of Tsukuba, Tsukuba, Ibaraki 305, Japan

Yoichi Kawakami, Shigeo Yamaguchi, Kunio Ichino, Shizuo Fujita, and Shigeo Fujita
Department of Electrical Engineering, Kyoto University, Kyoto 606-01, Japan

Tsunemasa Taguchi*
Department of Electrical Engineering, Osaka University, Suita, Osaka 565, Japan
 (Received 1 June 1994)

The radiative lifetime of biexcitons in $\text{Zn}_x\text{Cd}_{1-x}\text{Se-ZnS}_y\text{Se}_{1-y}$ multiple quantum wells has been studied by means of time-resolved luminescence spectroscopy under high-density excitation. It is shown that the rise of the biexciton luminescence becomes more rapid with increasing excitation energy density and that the biexciton luminescence decays with a double exponential form. It is found that the decay-time constant of the faster-decay component in the double-exponential decay corresponds to the radiative lifetime of the biexciton. Its value is about 6 ps at 2 K and is about one-seventh of that in bulk ZnSe (~ 40 ps).

It is now well established that two excitons interact attractively and form a bound state known as a biexciton (excitonic molecule). To date, there has been much work on biexciton formation in a large variety of semiconductors. In recent years, evidence for biexciton formation in GaAs-based quantum wells has also been reported.¹⁻³ In order to observe biexcitons in GaAs, it has been necessary to confine excitons in quantum wells, since in two dimensions the binding energy of the biexciton increases over the bulk value by nearly an order of magnitude.⁴ On the other hand, there has been only one report,⁵ to our knowledge, on biexciton formation in wide-band-gap II-VI quantum wells in spite of the advantages of excitonic nature: excitons and biexcitons in wide-band-gap II-VI semiconductors have much larger binding energies than those in III-V semiconductors.

We present here experimental evidence for biexciton formation in wide-band-gap II-VI multiple quantum wells (MQW's). Particularly, we demonstrate the temporal behavior of biexcitons under high-density excitation by employing time-resolved luminescence spectroscopy.

The sample used in this paper was prepared by metalorganic-molecular-beam epitaxy.⁶ The MQW layer was grown on a (100)-oriented GaAs substrate, following the deposition of a 50-nm-thick ZnSe buffer layer and an 800-nm-thick $\text{ZnS}_{0.08}\text{Se}_{0.92}$ cladding layer. The MQW structure consisted of six periods of 8-nm-thick $\text{Zn}_{0.83}\text{Cd}_{0.17}\text{Se}$ well layers separated by 10-nm-thick $\text{ZnS}_{0.08}\text{Se}_{0.92}$ barrier layers. A 170-nm-thick $\text{ZnS}_{0.08}\text{Se}_{0.92}$ cap layer was formed on top of the MQW structure.

The experiments were performed using a mode-locked titanium-sapphire laser and a titanium-sapphire regenerative amplifier, both of which were pumped by a cw Ar^+

laser. The repetition rate and the pulse width of the amplified-laser output were 250 kHz and 200 fs, respectively. The wavelength of the amplified-laser output can be tuned from 745 to 875 nm. The second harmonic light of the amplified-laser output was used as an excitation source. The time-resolved luminescence was measured by means of a synchroscan streak camera in conjunction with a subtractive-dispersion double monochromator. The instrumental response of this system had an exponential decay-time constant of about 5 ps.

Figure 1 shows the time-integrated luminescence spec-

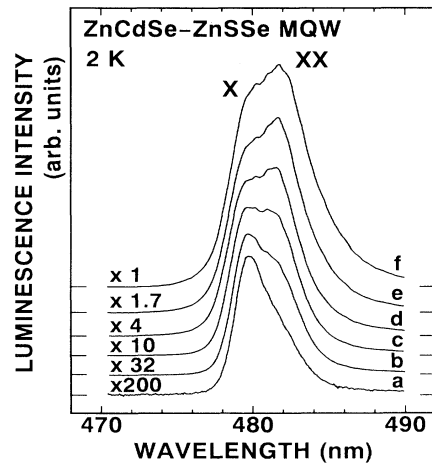


FIG. 1. Time-integrated luminescence spectra at 2 K taken from a $\text{Zn}_x\text{Cd}_{1-x}\text{Se-ZnS}_y\text{Se}_{1-y}$ MQW under excitation-energy densities of a, 0.3; b, 1.2; c, 3.0; d, 6.0; e, 18; and f, $49 \mu\text{J}/\text{cm}^2$. These spectra are shown after being multiplied by the number that is indicated on the left-hand side of each spectrum for clarity.

tra at 2 K taken from the MQW sample mentioned above under excitation-energy densities of *a*, 0.3; *b*, 1.2; *c*, 3.0; *d*, 6.0; *e*, 18; and *f*, 49 $\mu\text{J}/\text{cm}^2$. The excitation wavelength was 400 nm, which corresponded to band-to-band excitation. The luminescence at the low-excitation density shown in curve *a* is dominated by the radiative recombination of $n=1$ heavy-hole excitons (denoted by *X*), which shows the peak at 479.8 nm (2.583 eV). It is found from our separate experiments that the emission line of the $n=1$ heavy-hole exciton shows an almost symmetric line shape with a linewidth of approximately 12 meV under the lowest excitation by a cw He-Cd laser.⁷ On the other hand, under the short-pulsed excitation conditions, a shoulder appears on the low-energy side even at the low-excitation density less than 0.1 $\mu\text{J}/\text{cm}^2$. With increasing excitation-energy density, the shoulder grows more rapidly than the exciton line and becomes the dominant radiative-recombination process (denoted by *XX*), which shows the peak at 481.7 nm (2.573 eV).

On the basis of the spectral position, we attribute the line *XX* to the radiative recombination of biexcitons.⁸ The most frequent recombination process of biexcitons involves the annihilation of one electron-hole pair, leaving one exciton. This biexciton line follows the expected superlinear excitation-density dependence, and the dependence of the biexciton intensity on the exciton intensity gives approximately $I_{\text{biex}} \propto I_{\text{ex}}^{1.7}$. Then, the energy difference between the exciton and the biexciton lines is about 10 meV. Here, it is also found from our separate experiments that the difference in peak energy between the absorption and luminescence spectra of the $n=1$ heavy-hole exciton is as small as 5 meV.⁷ This energy difference, defined as a Stokes shift, results from the localization of excitons. On the other hand, such a localization effect on the biexciton is considered to be small because of the larger spatial extent of the biexciton than that of the exciton. Therefore, the binding energy of the biexciton in the quantum well can be estimated to be about 15 meV. This value is approximately four times as large as that in bulk ZnSe [3.5 meV (Ref. 9)]. The increase in the binding energy is clearly due to the effect of quantum confinement on the biexciton in the quantum well.

In order to confirm the above identification, the transient luminescence decay of the biexciton has been measured under various excitation-energy densities. Figure 2 shows the typical three time-resolved luminescences of the biexciton at 2 K taken from the MQW sample under excitation-energy densities of *a*, 6.0; *b*, 18; and *c*, 49 $\mu\text{J}/\text{cm}^2$. At the excitation-energy density as low as 6.0 $\mu\text{J}/\text{cm}^2$, the biexciton luminescence reaches the maximum intensity at about 50 ps after the excitation. Thereafter, it decays exponentially with a decay-time constant of about 140 ps. With increasing excitation-energy density, the rise of the biexciton luminescence becomes more rapid. In addition, a faster-decay component appears and it becomes prominent. As a result, the biexciton luminescence shows a double-exponential decay. Using a least-squares fit to the double-exponential decay as well as a deconvolution technique in consideration of the instrumental time resolution, the decay-time con-

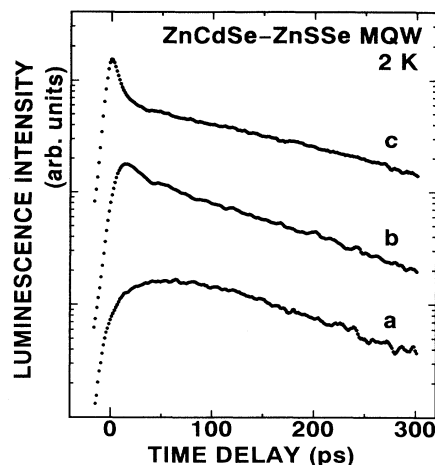


FIG. 2. Time-resolved luminescence of the biexciton in a $\text{Zn}_x\text{Cd}_{1-x}\text{Se-ZnS}_y\text{Se}_{1-y}$ MQW at 2 K under excitation-energy densities of *a*, 6.0; *b*, 18; and *c*, 49 $\mu\text{J}/\text{cm}^2$. The luminescence intensity is plotted on a logarithmic scale.

stants of the faster- and slower-decay components at 49 $\mu\text{J}/\text{cm}^2$ are estimated to be about 6 and 210 ps, respectively. At the excitation-energy densities above 49 $\mu\text{J}/\text{cm}^2$, these two values are found to be almost constant.

Furthermore, in order to identify the appearance of the faster-decay component as the characteristic of the biexciton luminescence itself, the transient decay at various positions of the luminescence band has been measured. Figure 3 shows the time-resolved luminescence at 2 K observed at *a*, 480.0; *b*, 481.0; *c*, 481.5; *d*, 482.0; *e*, 483.0; and *f*, 484.0 nm under the excitation-energy density of 49 $\mu\text{J}/\text{cm}^2$. It can clearly be seen from this figure that the faster-decay component appears only around the peak of the biexciton luminescence, which corresponds to the spectrum shown in Fig. 1(f). It is noted here that the peak of the biexciton luminescence (Fig. 3, curve *d*) occurs earlier than that of the exciton luminescence (Fig. 3, curve *a*). This experimental result means that the luminescence intensity of excitons reflects the total number of excitons in the sample whereas the biexciton formation is controlled by the density of electron-hole pairs.

The temporal behavior of biexcitons in bulk ZnSe has also been studied in order to compare the above-mentioned quasi-two-dimensional case with a three-dimensional case. Figure 4 shows the time-integrated luminescence spectra at 2 K taken from an ultrahigh-purity ZnSe bulk crystal under excitation-energy densities of *a*, 0.1; *b*, 0.6; *c*, 1.5; *d*, 6.2; and *e*, 52 $\mu\text{J}/\text{cm}^2$. The ZnSe bulk crystal was grown by a recrystallization traveling-heater method.¹⁰ The excitation wavelength was 400 nm, which corresponded to band-to-band excitation. At the excitation-energy density as low as 0.1 $\mu\text{J}/\text{cm}^2$, the luminescence spectrum is dominated by a free-exciton line associated with lower polaritons at 442.3 nm (denoted by *X*). It is noted here that there is no bound-exciton line associated with donor and acceptor impurities in this spectral range. This fact enables us to observe a biexciton line clearly. With increasing excitation-energy density, the biexciton line (denoted by

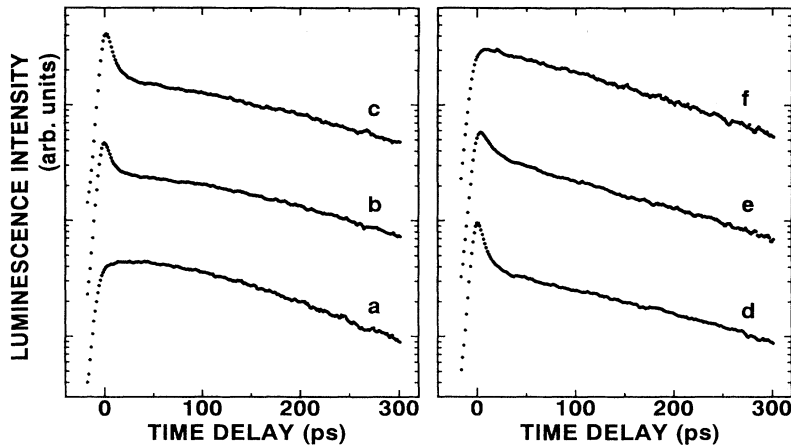


FIG. 3. Time-resolved luminescence at 2 K observed at *a*, 480.0; *b*, 481.0; *c*, 481.5; *d*, 482.0; *e*, 483.0; and *f*, 484.0 nm in a $\text{Zn}_x\text{Cd}_{1-x}\text{Se-ZnS}_y\text{Se}_{1-y}$ MQW under excitation-energy density of $49 \mu\text{J}/\text{cm}^2$. The luminescence intensity is plotted on a logarithmic scale.

XX) grows superlinearly (approximately $I_{\text{biex}} \propto I_{\text{ex}}^2$) and broadens to the lower-energy side as is clearly shown in Fig. 4. It can be seen from this figure that the biexciton line includes some fine structures. It has also been reported that five biexciton levels were observed by means of resonant Raman scattering under two-photon excitation of biexcitons.⁹ These assignments will be discussed elsewhere.

The transient luminescence decay of the biexciton line in bulk ZnSe is shown in Fig. 5. The excitation-energy densities were *a*, 0.9; *b*, 6.3; *c*, 15; *d*, 84; and *e*, $188 \mu\text{J}/\text{cm}^2$. At the excitation-energy density as low as $0.9 \mu\text{J}/\text{cm}^2$, the biexciton luminescence shows a slow rise and reaches the maximum intensity at about 250 ps after the excitation. Thereafter, it decays exponentially with a decay-time constant of about 530 ps. With increasing excitation-energy density, the rise of the biexciton luminescence becomes more rapid. In addition, a faster-decay component appears and it becomes prominent. As a result, the biexciton luminescence shows a double-exponential decay. The decay-time constant of the faster-decay component gradually becomes small and, on

the other hand, that of the slower-decay component becomes large with an increase in the excitation-energy density. Using the least-squares fit, the decay-time constants of the faster- and slower-decay components at $188 \mu\text{J}/\text{cm}^2$ are estimated to be about 40 and 680 ps, respectively. At the excitation-energy densities above $188 \mu\text{J}/\text{cm}^2$, these two values are found to be almost constant. This temporal behavior of the biexciton luminescence is similar to that observed in the MQW sample mentioned above.

It is reasonable to understand that the temporal behavior of the biexciton luminescence directly corresponds to the change in the total number of biexcitons. Then, the above results shown in Figs. 2 and 5 can qualitatively be explained as follows: At lower-excitation densities, excitons form initially following the creation of electron-hole pairs by optical excitation. Thereafter, biexcitons are formed as a result of the interaction between the two excitons. Therefore, the slow rise of the biexciton luminescence shown in curve *a* of Fig. 2 and curve *a* of Fig. 5 reflects the formation process of biexcitons from the excitons. The process of biexciton formation is very dependent on the density of excitons. At higher-

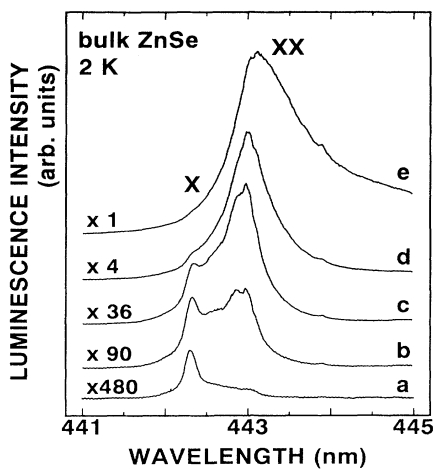


FIG. 4. Time-integrated luminescence spectra at 2 K taken from bulk ZnSe under excitation-energy densities of *a*, 0.1; *b*, 0.6; *c*, 1.5; *d*, 6.2; and *e*, $52 \mu\text{J}/\text{cm}^2$. These spectra are shown after being multiplied by the number that is indicated on the left-hand side of each spectrum for clarity.

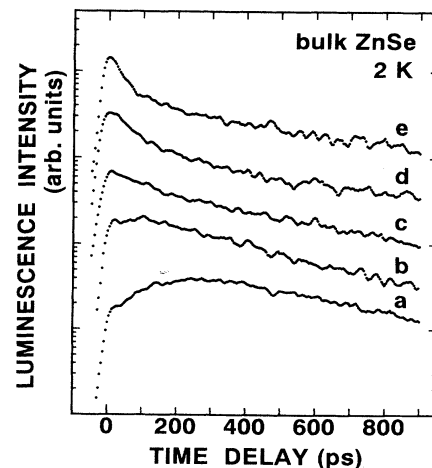


FIG. 5. Time-resolved luminescence of the biexciton in bulk ZnSe at 2 K under excitation-energy densities of *a*, 0.9; *b*, 6.3; *c*, 15; *d*, 84; and *e*, $188 \mu\text{J}/\text{cm}^2$. The luminescence intensity is plotted on a logarithmic scale.

excitation densities, on the other hand, the biexciton luminescence reaches the maximum intensity just after the excitation as shown in curve *c* of Fig. 2 and curve *e* of Fig. 5. The results mean that the biexciton formation takes place most efficiently just after the excitation. This is due to the increase in the formation rate of biexcitons caused by the exciton-exciton interaction as a result of the increase in the density of excitons. It may also be considered that the biexcitons are directly formed by the electron-hole pairs created initially by the optical excitation.

Very recently, such temporal behavior of biexciton luminescence under high-density band-to-band excitation has also been observed in nanometer-sized CuCl microcrystallites.¹¹ Then, the decay-time constant of the faster-decay component was interpreted as the radiative lifetime of biexcitons and the slower-decay component was explained by considering the recurring process between excitons and biexcitons: excitons reformed by the radiative annihilation of biexcitons form biexcitons again. Therefore, we can similarly consider that the decay-time constant of the faster-decay component, which is prominently observed at the higher-excitation densities as shown in curve *c* of Fig. 2 and curve *e* of Fig. 5, corresponds to the radiative lifetime of the biexcitons. Then, the radiative lifetime of the biexciton in the $\text{Zn}_x\text{Cd}_{1-x}\text{Se}$ MQW and that in the bulk ZnSe are obtained to be about 6 and 40 ps, respectively, by means of the least-squares fit to the double-exponential decay and the deconvolution technique as already mentioned above. On the basis of the fact that oscillator strength is proportional to the reciprocal of the radiative lifetime, the above experimental results mean that the oscillator strength for the transition between the biexciton and exciton states in the $\text{Zn}_x\text{Cd}_{1-x}\text{Se}$ quantum well increases by a factor of about 7 in comparison with that in the bulk ZnSe.

On the other hand, the decay-time constant of the slower-decay component of the biexciton luminescence in the bulk ZnSe is about 680 ps as shown in curve *e* of Fig. 5. This value is approximately half of the radiative lifetime of free excitons, 1300 ps, which is determined by the radiative lifetime of the LO-phonon-assisted free excitons

($X-1\text{LO}$) in order to avoid a polariton effect. This fact can easily be explained by considering the recurring process between excitons and biexcitons, in which the total number of biexcitons is proportional to the square of that of excitons. The slower-decay component of the biexciton luminescence observed in the MQW ($\tau_d \sim 210$ ps) can also be explained similarly. On the basis of the above experimental results, it is found that the exciton oscillator strength in the $\text{Zn}_x\text{Cd}_{1-x}\text{Se}$ quantum well increases by a factor of about 4 in comparison with that in the bulk ZnSe. In the case of a ZnSe quantum well with the same well layer thickness of 8.0 nm and infinite potential height, the exciton oscillator strength is found from calculation to be 4.1 times as large as that in the bulk ZnSe. Therefore, we consider that the experimental results are well supported by the calculated results though the quantum-well layer is not ZnSe, but $\text{Zn}_x\text{Cd}_{1-x}\text{Se}$. However, there is little theoretical consideration about the oscillator strength for the transition between the biexciton and exciton states in the quantum well.

In conclusion, we have studied the time-resolved luminescence of the biexcitons in the $\text{Zn}_x\text{Cd}_{1-x}\text{Se}-\text{ZnS}_y\text{Se}_{1-y}$ multiple quantum wells under high-density excitation. With increasing excitation-energy density, the rise of the biexciton luminescence became more rapid. In addition, the biexciton luminescence showed the double-exponential decay and the decay-time constant of the faster-decay component was attributed to the radiative lifetime of the biexcitons. On the other hand, the slower-decay component was explained by considering the recurring process between the biexcitons and excitons. The above experimental results were compared with that for the bulk ZnSe. It was shown that the oscillator strength for the transition between the biexciton and exciton states in the $\text{Zn}_x\text{Cd}_{1-x}\text{Se}$ quantum well increased by a factor of about 7 in comparison with that in the bulk ZnSe.

The authors would like to thank Professor Tetsuo Ogawa of Osaka City University for valuable discussions. This work was partly supported by the Iketani Science and Technology Foundation.

*Present address: Department of Electrical and Electronic Engineering, Faculty of Engineering, Yamaguchi University, Tokiwadai 2557, Ube 755, Japan.

¹R. C. Miller, D. A. Kleinman, A. C. Gossard, and O. Munteanu, *Phys. Rev. B* **25**, 6545 (1982).

²D. J. Lovering, R. T. Phillips, G. J. Denton, and G. W. Smith, *Phys. Rev. Lett.* **68**, 1880 (1992).

³R. T. Phillips, D. J. Lovering, G. J. Denton, and G. W. Smith, *Phys. Rev. B* **45**, 4308 (1992).

⁴D. A. Kleinman, *Phys. Rev. B* **28**, 871 (1983).

⁵Q. Fu, D. Lee, A. Mysyrowicz, A. V. Nurmikko, R. L. Gunshor, and L. A. Kolodziejski, *Phys. Rev. B* **37**, 8791 (1988).

⁶Y.-h. Wu, Y. Kawakami, Sz. Fujita, and Sg. Fujita, *Jpn. J. Appl. Phys.* **30**, L555 (1991).

⁷S. Yamaguchi, T. Shinzato, K. Ichino, Y. Kawakami, Sz. Fujita, and Sg. Fujita, *J. Lumin.* **59**, 341 (1994).

⁸It is noted here that the stimulated emission from the same MQW sample was observed at 483.8 nm (2.562 eV) using the same excitation-laser system. This position is located at about the 11-meV lower-energy side of the peak of the biexciton luminescence (line *XX*). Therefore, it is clear that the line *XX* is not due to the excitonic-gain process.

⁹Y. Nozue, M. Itoh, and K. Cho, *J. Phys. Soc. Jpn.* **50**, 889 (1981).

¹⁰T. Taguchi, I. Kidoguchi, and H. Namba, U.S. Patent No. 4,866,007.

¹¹Y. Masumoto, S. Katayanagi, and T. Mishina, *Phys. Rev. B* **49**, 10 782 (1994).